

Hyperfine structure of hydrogenlike thallium isotopes

Peter Beiersdorfer, Steven B. Utter,* Keith L. Wong, José R. Crespo López-Urrutia,† Jerry A. Britten, Hui Chen, Clifford L. Harris,‡ Robert S. Thoe, Daniel B. Thorn, and Elmar Träbert§
Lawrence Livermore National Laboratory, Livermore, California 94550

Martin G. H. Gustavsson, Christian Forssén, and Ann-Marie Mårtensson-Pendrill
Physics and Engineering Physics, Göteborg University and Chalmers University of Technology, SE-412 96 Göteborg, Sweden
(Received 13 February 2001; published 20 August 2001)

The hyperfine splitting of the $1s$ ground state of hydrogenlike Tl has been measured for the two stable isotopes using emission spectroscopy in the SuperEBIT electron-beam ion trap, giving 3858.22 ± 0.30 Å for $^{203}\text{Tl}^{80+}$ and 3821.84 ± 0.34 Å for $^{205}\text{Tl}^{80+}$ with a wavelength difference $\Delta\lambda = 36.38 \pm 0.35$ Å. This difference is consistent with estimates based on hyperfine anomaly data for neutral Tl only if finite size effects are included in the calculation. By using previously determined nuclear magnetic moments, and applying appropriate corrections for the nuclear charge distribution and radiative effects, the experimental splittings can be interpreted in terms of nuclear magnetization radii $\langle r_m^2 \rangle^{1/2} = 5.83(14)$ fm for ^{203}Tl and $\langle r_m^2 \rangle^{1/2} = 5.89(14)$ fm for ^{205}Tl . These values are 10% larger than derived from single-particle nuclear magnetization models, and are slightly larger than the corresponding charge distributions.

DOI: 10.1103/PhysRevA.64.032506

PACS number(s): 32.10.Fn, 32.30.Jc, 31.30.Gs, 21.10.Gv

I. INTRODUCTION

The hyperfine structure (HFS) of highly charged hydrogenlike systems challenges experimental techniques as well as our understanding of the details in the description of the $1s$ electron and its interaction with the nucleus. Radiative corrections are of the order 0.5%, observable within the experimental uncertainty of accurate spectroscopic investigations, and even higher-order radiative corrections may be in reach for these extremely relativistic systems [1,2]. The remaining electron is a good probe of the bare nucleus, as the electronic wave function is sensitive to details in the nuclear charge distribution and the resulting HFS also depends on the unknown magnetization distribution. These effects are also present for neutral systems, where they are, however, obscured by many-electron interactions and only “hyperfine anomalies” can be accurately determined. These are isotopic differences in the ratio between the A factor for the hyperfine structure and the nuclear g_I factor (where $g_I = \mu_I / I\mu_N$).

Measurements of HFS for highly charged hydrogenlike systems have been reported for several elements: $^{165}\text{Ho}^{66+}$ [3], $^{185}\text{Re}^{74+}$ [4], $^{187}\text{Re}^{74+}$ [4], $^{207}\text{Pb}^{81+}$ [5], $^{209}\text{Bi}^{82+}$ [6], and $^{209}\text{Bi}^{80+}$ [7]. The results, in particular for $^{165}\text{Ho}^{66+}$ and $^{185,187}\text{Re}^{74+}$, were found to differ considerably from predictions based on a single-nucleon description for the nuclear magnetization [8–10]. For the case of Tl, which is closer to a double-magic nucleus, better agreement should be expected. In addition, the hyperfine anomaly for neutral Tl, can

be used to predict the isotopic difference in HFS for the hydrogenlike systems [10].

In the following, we present a measurement of the $1s$ hyperfine splitting of the two stable isotopes of thallium, hydrogenlike $^{203}\text{Tl}^{80+}$, and $^{205}\text{Tl}^{80+}$. Using a spectrometer with greatly enhanced sensitivity and resolving power, we have achieved a measurement accuracy that is between four and eight times better than our earlier measurements of the hyperfine splitting in $^{165}\text{Ho}^{66+}$, $^{185}\text{Re}^{74+}$, and $^{187}\text{Re}^{74+}$ [3,4], and has twice the accuracy of laser-fluorescence measurements of $^{209}\text{Bi}^{82+}$ and $^{207}\text{Pb}^{81+}$ carried out on the ESR storage ring [5,6].

The experimentally determined HFS results thus obtained are used to determine absolute values for the nuclear magnetization radii of the two isotopes, by using known magnetic moments and charge radii and calculated radiative corrections, as discussed in Sec. V.

II. EXPERIMENT

As with our earlier measurements [3,4], the thallium measurements were carried out at the SuperEBIT electron-beam ion trap [11] at the Lawrence Livermore National Laboratory. This was the first experiment after an 18-month shutdown, and SuperEBIT could not be operated at full capacity. The electron-beam currents varied between 180 and 240 mA. The electron-beam energy was set to 142 keV, which is about $1.5\times$ the energy necessary to produce hydrogenic thallium.

The resulting charge balance was somewhat worse than that during our rhenium measurements [4], as could be estimated from hard x-ray measurements of the radiative electron capture into the $1s$, $2s$, and $2p$ levels of various thallium ions. The amount of hydrogenic thallium, for example, was estimated to be less than 2%.

The $F=1 \rightarrow F=0$ $1s$ hyperfine transition in either thallium isotope is predominately excited by ionizing collisions with heliumlike thallium. The reason is that ionization of a

*Present address: Spectra-Physics, Mountain View, CA 94043.

†Present address: Fakultät für Physik, Albert-Ludwigs-Universität Freiburg, Germany.

‡Permanent address: Department of Physics, University of Nevada, Reno, Nevada.

§Also at Fakultät für Physik und Astronomie, Ruhr-Universität Bochum, Germany and IPNAS, Université de Liège, Belgium.

$1s$ electron from the $1s^2 \ ^1S_0$ heliumlike ground level populates the $1s$ hyperfine levels in a statistical fashion, i.e., the population ratio of the $F=1$ upper level to that of the $F=0$ lower level is 3:1. The rates for electron-impact excitation or excitation of the $F=1$ level by radiative electron capture are negligible by comparison. In a steady state, electron-impact ionization is balanced by radiative recombination. Consequently, monitoring the x rays emitted by the latter process gives us a measure of the ionization process and thus of the amount of photons emitted by the hyperfine decay. As a result, our experiment aimed at maximizing the amount of hydrogenic thallium and was hurt by the fact that we could not achieve a better charge balance during the 5 months (including startup) of this experiment.

Our experiment benefited greatly from a new spectrometer designed specifically for this measurement. Instead of a prism as used previously [3,4], the new instrument utilized a 6-in.-diam quartz transmission grating and two 13-cm diameter $f/4.6$ quartz lenses for one-to-one imaging of the source onto a cryogenically cooled scientific-grade Photometrics charge-coupled device (CCD) camera. The grating was built in house, with 2857 lines/mm and a near 90% efficiency at the wavelengths of interest [12]. This instrument had been used to measure the optical transition in Ti-like W^{52+} in preparation for the present experiment [13]. A second instrument of almost the same design parameters was temporarily used in parallel in order to increase the signal rate. However, due to the higher intrinsic noise level of its CCD camera chip, this detection branch failed.

A wavelength region 130 Å wide could be measured with the instrument in one setting. Three settings were used to scan (with overlap) a 300 Å wide region centered at 3800 Å during a ten-week period. This region covered the wavelength range suggested by various predictions, which range from 3786 to 3802 Å for $^{203}\text{Tl}^{80+}$, and 3822 to 3840 Å for $^{205}\text{Tl}^{80+}$ [8–10]. For each setting we measured spectra with and without thallium injection to gauge the emission from background ions. In both cases, we introduced argon as a cooling gas, setting the ballistic gas injector pressure to 1×10^{-8} Torr. We also measured argon directly by setting the gas injector pressure to 5×10^{-7} Torr. The presence of any potential heavy contaminants during the argon-only measurements was avoided by emptying the trap about four times per second. For the thallium and background measurements the trap was emptied about once every minute. In order to minimize read-out noise, each spectrum accumulated for 1 h before the camera was read out.

Argon provided the reference lines for the spectral calibration. At the high injector pressure, faint lines of argon could be seen within a single, 1 h spectrum. Also seen were sharp spikes from cosmic-rays events, which were filtered out using the “bad-pixel” routine in the IPLab imaging software on a Macintosh G3 computer. A 63 h argon spectrum is shown in Fig. 1 (lower trace). In contrast to the argon spectra, a 1 h spectrum of the SuperEBIT emission with thallium injection or from low-argon background ions showed no lines or features at all after the cosmic rays were filtered out. In fact, we rejected any spectra taken while thallium was injected that showed any discernible features, as those were

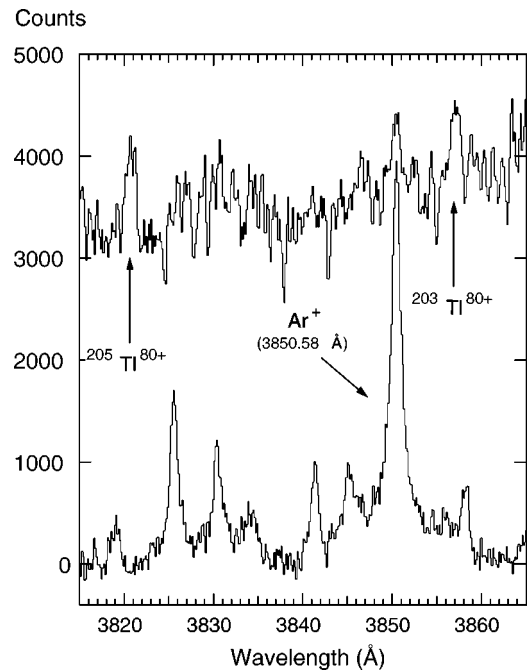


FIG. 1. Experimental spectrum of H-like thallium (upper trace) with the hyperfine transitions in the two Tl isotopes indicated. The lower trace is the reference spectrum of argon. An arbitrary offset is used to separate the two traces.

thought to arise from inadequate filtering of cosmic rays. About 30 individual spectra were then added and examined for features. A spectrum resulting from adding 194 1 h spectra with thallium injection is shown in Fig. 1 (upper trace).

III. RESULTS

The argon lines seen in the lower trace of Fig. 1 are mostly due to singly ionized argon. These lines have been measured to a very high accuracy [14] so that they represent excellent reference lines. Not all lines can be identified. In fact, most weak lines are unknown, as pointed out in Ref. [15]. There is a sufficient number of strong Ar^+ lines that can be identified and used to determine the absolute wavelength scale and the dispersion. These include the line at 3850.581 Å shown in Fig. 1, as well as others at 3946.097, 3868.528, and 3809.456 Å.

Argon lines are also seen weakly in the thallium measurements and in the background spectra. In fact, these built-in calibration lines help to maintain the integrity of the wavelength calibration over days of measurements. Shifts in the position of the argon lines, possibly caused by temperature variations, have been noted on a time scale of a day. In fact, such shifts have limited the accuracy of the Ti-like W^{52+} measurement mentioned above [13].

The identification of the thallium lines was not without hesitation. The spectrum in Fig. 1 was the best we could do under the measurement conditions. The two features labeled by the respective thallium isotope are the only features that satisfy the following criteria: they are found in the thallium injection spectra, are missing in the background spectra, and cannot be correlated with any argon lines. These criteria, plus

TABLE I. Summary of uncertainties affecting the wavelength determination of the hyperfine transitions.

Source	$^{203}\text{Tl}^{80+}$	$^{205}\text{Tl}^{80+}$
Tl line position	0.21 Å	0.21 Å
Calibration line position	0.21 Å	0.21 Å
Dispersion	0.02 Å	0.12 Å
Edge nonlinearity	0.00 Å	0.12 Å
Quadrature sum	0.30 Å	0.34 Å

the fact that their wavelength separation is very close to the predicted value, lead us to identify the two lines as the sought-after hyperfine transitions from $^{203}\text{Tl}^{80+}$ and $^{205}\text{Tl}^{80+}$.

The two thallium features are statistically poor. The ratio of ^{203}Tl to ^{205}Tl in natural thallium, which we used for injection, is about 3:7. This is difficult to ascertain in the observed intensity ratio, though it is not in contradiction either. Despite the poor statistics, we note that the widths of the thallium lines are only 1.1 Å. This is more than ten times less than the line we observed in Ho^{66+} using a prism spectrometer, and this clearly demonstrates the technical improvement.

We estimate that we can determine the centroid of each line to within 20% of its width. We assume a similar accuracy for the argon lines used to check for spectral shifts. The uncertainties in the spectral dispersion are small for the ^{203}Tl line, which is close to one of the calibration lines. They are larger for the ^{205}Tl line. The latter line is also close to the edge of the CCD chip, and we take into account possible edge nonlinearities. A summary of the uncertainties affecting each line is given in Table I. Adding them in quadrature, we obtain 3857.13 ± 0.30 Å for the wavelength of the $^{203}\text{Tl}^{80+}$ hyperfine transition, and 3820.76 ± 0.34 Å for the wavelength of the $^{205}\text{Tl}^{80+}$ hyperfine transition. The $1-\sigma$ accuracy of the present measurement is about an order of magnitude worse than one could expect from the nominal resolving power of the instrument and in the absence of significant systematic errors.

Converting our results to vacuum wavelengths, we get 3858.22 ± 0.30 and 3821.84 ± 0.34 Å, and a corresponding energy splitting of $3.213\,50 \pm 0.000\,25$ and $3.244\,09 \pm 0.000\,29$ eV, respectively.

The isotopic difference in the hyperfine splittings is obtained by subtracting the wavelengths of the two transitions. The result is 36.38 ± 0.35 Å, or 30.59 ± 0.29 meV. The uncertainties are determined by noting that the uncertainty in the calibration line drops out when subtracting the two wavelengths, while the uncertainties arising from the wavelength dispersion (cf. Table I) add linearly.

IV. THEORY: ONE-ELECTRON SYSTEMS AND HYPERFINE STRUCTURE

The Dirac equation for hydrogenlike systems with a pointlike nucleus is a standard textbook example. For heavy

elements, however, it is essential to use the potential from an extended nuclear charge distribution in the Dirac equation for the electron. In this paper we use a Fermi model for the nuclear distribution using the $\langle r_c^2 \rangle^{1/2}$ values 5.463(5) fm for ^{203}Tl and 5.470(5) fm for ^{205}Tl obtained from elastic electron scattering and muonic x-ray data [16,17], and a skin thickness parameter $a = 0.524(10)$ fm.

The interaction between the electron and point nuclear magnetic dipole moment $\boldsymbol{\mu}_I = g_S \mathbf{S}_N + g_L \mathbf{L}_N$ of a nucleus (with $I \neq 0$) can be described by a Hamiltonian

$$h_p^{\text{HFS}} = \frac{\mu_0}{4\pi} ec \frac{\hat{\mathbf{r}} \times \boldsymbol{\alpha}}{r^2} \cdot \boldsymbol{\mu}_I. \quad (1)$$

The hyperfine interaction in Eq. (1) holds only for a point nuclear dipole. For an extended magnetization, the radial function $1/r^2$ is modified inside the nucleus. The general expression depends on the combination of spin and angular momentum contributions to the nuclear magnetic moment. For the stable Tl isotopes with $I = 1/2^+$, only the spin magnetic moment enters. For a spin magnetic moment on a shell, the interaction vanishes when the electron is inside the shell. The interaction for a general distribution of magnetic moment can, of course, be obtained by integration, giving a Bohr-Weisskopf correction factor $(1 - \varepsilon_{\text{BW}})$, where

$$\varepsilon_{\text{BW}} = a_2 \langle r_m^2 \rangle + a_4 \langle r_m^4 \rangle + a_6 \langle r_m^6 \rangle. \quad (2)$$

For Tl, we find $a_2 = 7.6 \times 10^{-4} \text{ fm}^{-2}$, $a_4 = -3.1 \times 10^{-6} \text{ fm}^{-4}$, and $a_6 = 7.3 \times 10^{-9} \text{ fm}^{-6}$ [10,18] for hydrogenlike Tl. An important observation from the analytical expansions is that ε_{BW} depends on the angular momentum of the electron, but is essentially independent of the principal quantum number, since the correction depends on the radial dependence of the orbital in a region where the nuclear potential is very large compared to the differences in binding energy. This essential n independence makes it possible to use hyperfine anomaly results from neutral systems to obtain estimates of the anomaly for hydrogenlike systems, although for neutral atoms, modifications due to the interactions with the other electrons must be accounted for, as discussed in more detail below. For further details, see [19].

A. Radiative corrections

The strong electromagnetic field close to the nucleus leads to radiative effects also modifying the interaction with the nuclear magnetic moment. The sizes of these effects were evaluated by Sunnergren *et al.* [20,21] using the numerical orbitals obtained in the potential from a Fermi charge distribution, giving $\Delta E_{\text{QED}}/\mu_I = -0.011\,14(11)$ eV/ μ_N for both isotopes.

B. Single-particle estimates of the Bohr-Weisskopf effect

The evaluation of expression (2) for the Bohr-Weisskopf effect requires an approximation for the distribution of nuclear magnetization. In earlier work we used a Woods-Saxon potential [10,18] for the $3s$ proton hole. For ^{205}Tl the resulting parameters were $\langle r^2 \rangle^{1/2} = 5.27$ fm, $\langle r^4 \rangle^{1/4}$

TABLE II. Relevant parameters for the two stable Tl isotopes. The last three columns present experimental results from this paper, as well as the extracted Bohr-Weisskopf effect and the magnetization radii.

	$\mu_I^{\text{uncorr}}/\mu_N^a$	$\mu_I^{\text{corr}}/\mu_N^b$	$\langle r_c^2 \rangle^{1/2c}$ (fm)	$\Delta E_{\text{p.d.}}/\mu_I$ (eV/ μ_N)	$\Delta E_{\text{QED}}/\mu_I^d$ (eV/ μ_N)	$\Delta E_{\text{HFS}}^{\text{exp}}$ (eV)	ε	$\langle r_m^2 \rangle^{1/2}$ (fm)
$^{203}\text{Tl}^{80+}$	1.595 7681(1)	1.6217(13)	5.463(5)	2.0378(2)	-0.011 14(11)	3.213 51(25)	0.0221(8)	5.83(14)
$^{205}\text{Tl}^{80+}$	1.611 4643(1)	1.6379(13)	5.470(5)	2.0376(2)	-0.011 14(11)	3.244 09(29)	0.0225(8)	5.89(14)
Ratio	1.009 836 13(6)					1.009 52(12)		

^aNMR result by Baker and Burd, Ref. [26], not corrected for diamagnetic shielding and chemical shift.

^bReference [25], based on ABMR data for free atoms by Fowler, Ref. [33], corrected for diamagnetic shielding.

^cReference [17].

^dReference [20].

= 6.01 fm, and $\langle r^6 \rangle^{1/6} = 6.44$ fm (and $\langle r^2 \rangle = 27.8$ fm²). Other calculations, using different single-particle models [9,22], give $\langle r^2 \rangle$ values between 27.4 and 28.9 fm², all smaller than the corresponding radius of the total charge distribution.

Using our calculated $3s$ distribution gives $\varepsilon = 1.74(52)\%$, where the large uncertainty reflects the neglect of nuclear many-body effects. Combination with previously calculated radiative corrections gives $\Delta E_{\text{HFS}}/\mu_I = 1.9912(2)$ eV/ μ_N for the ground state of hydrogenlike ^{203}Tl and a slightly smaller value, $1.9910(2)$ eV/ μ_N for ^{205}Tl , which is known to have a slightly more extended charge distribution; $\delta\langle r_c^2 \rangle = 0.115(3)$ fm² [23,24].

In order to convert these results to expected hyperfine splittings, values for the nuclear magnetic moments must be inserted. As discussed in Ref. [25], diamagnetic shielding corrections must be applied to the tabulated nuclear magnetic resonance (NMR) values [26,27], giving the revised values shown in Table II. Adding radiative corrections from Sunnergren *et al.* [20,21] leads to the values $\Delta E_{\text{HFS}}^{203} = 3.229(17)$ eV and $\Delta E_{\text{HFS}}^{205} = 3.261(18)$ eV [10], somewhat larger than the experimentally observed splittings.

C. Isotopic differences for hydrogenlike and neutral systems: Differences and similarities

The different magnetic moments for the two Tl isotopes account for most of the 30.59(38) meV difference between the splittings. However, the ratio $\Delta E_{\text{HFS}}(^{205}\text{Tl})/\Delta E_{\text{HFS}}(^{203}\text{Tl}) = 1.009 52(12)$ between the observed splittings, differs slightly from the known ratio between the nuclear magnetic moments [26], $\mu_I(^{205}\text{Tl})/\mu_I(^{203}\text{Tl}) = 1.009 836 13(6)$. The resulting ‘‘hyperfine anomaly’’ can be written as

$$^{203}\Delta^{205} = (\Delta E_{\text{HFS}}^{203}/\Delta E_{\text{HFS}}^{205})(\mu_I^{205}/\mu_I^{203}) - 1.$$

Inserting the experimental values gives the hyperfine anomaly $^{203}\Delta^{205} = -3(1) \times 10^{-4}$, which accounts for about 1 meV of the difference between the hyperfine splittings of the two isotopes.

The hyperfine anomaly for the ground state of hydrogenlike Tl can be more accurately estimated by using anomalies for neutral Tl, measured in the early days of radio frequency

spectroscopy. For the $6p_{1/2}$ ground state of neutral Tl, the anomaly is $-1.036(3) \times 10^{-4}$ [28]. Many-body effects were found to account for about 9% of the total $6p_{1/2}$ anomaly [29]. To estimate the size of the $1s$ anomaly for the hydrogenlike system, we recall that a one-electron anomaly is essentially n independent, but varies with angular momentum. The ratio between the Bohr-Weisskopf effect for the $s_{1/2}$ and $p_{1/2}$ orbitals is about 3.3. The total anomaly is, however, also affected by the nuclear charge distribution, which affects the orbitals close to the nucleus. The ratio between this ‘‘Breit-Rosenthal(-Crawford-Schawlow)’’ effect for $s_{1/2}$ and $p_{1/2}$ orbitals is slightly larger, 3.7. The ratio between the anomalies for $s_{1/2}$ and $p_{1/2}$ thus depends on the relative importance of changes in the nuclear charge and magnetization distributions.

By performing calculations for several different Fermi distributions, the ‘‘Breit-Rosenthal’’ effect [30–32], which is expressed in terms of a correction factor $(1 - \varepsilon_{\text{BR}})$, can be parametrized in terms of changes in the charge distribution, using $\varepsilon_{\text{BR}} = -x_r \delta\langle r_c^2 \rangle$ (neglecting any changes in the skin thickness). For the ground state of hydrogenlike Tl we found in earlier work $x_r = -1.16 \times 10^{-3}$ fm⁻² [10,18]. This value was obtained by using the hyperfine interaction from a point dipole. The interaction with an extended magnetic dipole moment, however, gives less weight to the electron orbital for very small radii. As a result, the sensitivity to the nuclear charge distribution is reduced if the interaction with an extended dipole is considered, as illustrated in Fig. 2. This leads to a revised parametrization: $x_r = -0.78 \times 10^{-3}$ fm⁻² for the $1s$ ground state of hydrogenlike Tl.

For $6p_{1/2}$, the reduced sensitivity to the charge distribution also affects the earlier interpretation for neutral Tl [29]. The revised contribution due to the charge distribution is $-0.245(6) \times 10^{-4}$ of the total anomaly resulting in a slightly modified value for the change in magnetization radius, $\lambda_m = 0.299(5)$ or $\delta\langle r_m^2 \rangle = 0.38(1)$ fm².

Following these considerations, the data from the $6p_{1/2}$ ground state of neutral Tl yield an estimate of $-3.21(5) \times 10^{-4}$ for the anomaly of the $1s$ ground state of hydrogenlike Tl, corresponding to an energy difference of 30.71 ± 0.16 meV or a wavelength difference of 36.17 ± 0.19 Å, in excellent agreement with the measurement.

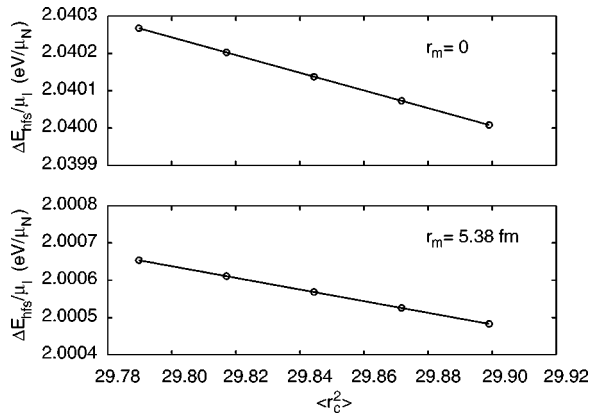


FIG. 2. Sensitivity of the hyperfine splitting to $\langle r_c^2 \rangle$ for the point-dipole and the magnetic dipole moment on a shell with radius 5.38 fm.

V. INTERPRETING THE EXPERIMENTAL DATA

The experimental hyperfine splittings are smaller than expected from the Woods-Saxon estimates [8–10], indicating that the actual nuclear magnetization distribution is more extended. The extracted Bohr-Weisskopf corrections are 2.212(81)% and 2.248(81)% for $^{203}\text{Tl}^{+81}$ and $^{205}\text{Tl}^{+81}$, respectively. Following the procedure described in Ref. [4], these values can be converted to magnetization radii of $\langle r_m^2 \rangle^{1/2} = 5.83(14)$ fm for ^{203}Tl and $\langle r_m^2 \rangle^{1/2} = 5.89(14)$ fm for ^{205}Tl . In contrast to the Woods-Saxon results, these radii are larger than the corresponding charge radii, indicating the importance of nuclear many-body effects.

The size of the magnetic moment distribution can be taken as an indication of the distribution of a possible P and T violating nuclear electric dipole moment, which, to a first approximation, can be expected to follow the valence nucleon, just like the magnetic moment. The higher-order corrections depend, however, on the angular structure of the operator, and cannot be immediately applied for other properties.

VI. CONCLUSION

Measurements of the $1s$ hyperfine splitting in muonic thallium found 2.30 ± 0.02 keV for ^{205}Tl and 2.34 ± 0.08 keV for ^{203}Tl [23]. The muonic measurements already showed the need to include the finite-nuclear-size in the calculations of the hyperfine splitting. This inclusion reduced the calculated value by half.

The present measurements of the electronic hyperfine splitting are about two orders of magnitude more accurate than the muonic measurements and enable tests of the detailed nuclear structure. Using our measured values, an rms nuclear magnetic radius of 5.83 ± 0.14 and 5.89 ± 0.14 fm can be inferred for the thallium isotopes 203 and 205, respectively. These values are about 7% larger than the single-particle estimate of 5.27 ± 0.74 fm [10,18], showing that the magnetization distribution is more extended than the charge distribution.

The measured isotope difference of 30.59 ± 0.38 meV differs slightly from the value of 31.04 ± 0.01 meV, inferred from neutral thallium using a point magnetic dipole approximation [10]. This difference lead us to consider a parametrization of the Breit-Rosenthal effect in terms of changes in the charge distribution for an extended magnetic dipole. Our calculations showed a significant reduction in the sensitivity to changes in the nuclear charge distribution, as the value of x_r dropped by about 33%. The resulting prediction for the isotopic difference of 30.71 ± 0.16 meV is now in excellent agreement with the measurement.

The present measurements were performed using emission spectroscopy on the Livermore SuperEBIT device. Although the accuracy exceeded that of past measurements, including those employing laser fluorescence, it was limited by the low production of hydrogenlike thallium ions. Improvements in hydrogenlike ion production, as SuperEBIT regains full operation, will undoubtedly improve the accuracy further in future measurements.

ACKNOWLEDGMENTS

The experimental work was performed under the auspices of the U.S. Department of Energy by the University of California Lawrence Livermore National Laboratory under Contract No. W-7405-ENG-48. We gratefully acknowledge support from E. Röhlfing and the Chemical Sciences, Geosciences, and Biosciences Division of the Office of Basic Energy Sciences, Office of Science, U.S. Department of Energy. We thank M. Tomaselli and Th. Kühl for discussions and communications concerning new calculations they have done. M.G.H.G., C.F., and A.-M.M.-P. would also like to express their appreciation of helpful discussions with the atomic physics and subatomic physics groups at Göteborg. Financial support from the Swedish Natural Science Research Council (NFR) and the Eurotraps EU-TMR Network is gratefully acknowledged. E.T. thankfully acknowledges support from DFG (Germany) and FNRS (Belgium).

- [1] B. Franzke, Nucl. Instrum. Methods Phys. Res. B **24/25**, 18 (1987).
 [2] T. Kühl, Phys. Scr. **T22**, 144 (1988).
 [3] J.R. Crespo López-Urrutia, P. Beiersdorfer, D.W. Savin, and K. Widmann, Phys. Rev. Lett. **77**, 826 (1996).
 [4] J.R. Crespo López-Urrutia, P. Beiersdorfer, K. Widmann, B.B. Birkett, A.-M. Mårtensson-Pendrill, and M.G.H. Gustavsson, Phys. Rev. A **57**, 879 (1998).

- [5] P. Seelig, S. Borneis, A. Dax, T. Engel, S. Faber, M. Gerlach, C. Holbrow, G. Huber, T. Kühl, D. Marx, K. Meier, P. Merz, W. Quint, F. Schmitt, M. Tomaselli, L. Völker, H. Winter, M. Würtz, K. Beckert, B. Franzke, F. Nolden, H. Reich, M. Steck, and T. Winkler, Phys. Rev. Lett. **81**, 4824 (1998).
 [6] I. Klaft, S. Borneis, T. Engel, B. Fricke, R. Grieser, G. Huber, T. Kühl, D. Marx, R. Neumann, S. Schröder, P. Seelig, and L. Völker, Phys. Rev. Lett. **73**, 2425 (1994).

- [7] P. Beiersdorfer, A.L. Osterheld, J.C. Scofield, J.R. Crespo López-Urrutia, and K. Widmann, *Phys. Rev. Lett.* **80**, 3022 (1998).
- [8] V.M. Shabaev, *J. Phys. B* **27**, 5825 (1994).
- [9] V.M. Shabaev, M. Tomaselli, T. Kühn, A.N. Artemyev, and V.A. Yerokhin, *Phys. Rev. A* **56**, 252 (1997).
- [10] M.G.H. Gustavsson, C. Forssén, and A.-M. Mårtensson-Pendrill, *Hyperfine Interact.* **127**, 347 (2000).
- [11] D.A. Knapp, R.E. Marrs, S.R. Elliott, E.W. Magee, and R. Zasadzinski, *Nucl. Instrum. Methods Phys. Res. A* **334**, 305 (1993).
- [12] H.T. Nguyen, B.W. Shore, S.J. Bryan, J.A. Britten, R.D. Boyd, and M.D. Perry, *Opt. Lett.* **22**, 142 (1997).
- [13] S.B. Utter, P. Beiersdorfer, and G.V. Brown, *Phys. Rev. A* **61**, 030503(R) (2000).
- [14] NIST Atomic Spectra Database, Version 2.0, <http://physics.nist.gov/PhysRefData/>
- [15] H. Chen, P. Beiersdorfer, C. L. Harris, and S. B. Utter (unpublished).
- [16] H. Euteneuer, J. Friedrich, and N. Voegler, *Nucl. Phys. A* **298**, 452 (1978).
- [17] H. de Vries, C.W. de Jager, and C. de Vries, *At. Data Nucl. Data Tables* **36**, 495 (1987).
- [18] C. Forssén, Master's thesis, Physics and Engineering Physics, Göteborg University and Chalmers University of Technology, 1998.
- [19] M. G. H. Gustavsson, Ph.D. thesis, Physics and Engineering Physics, Göteborg University and Chalmers University of Technology, 2000.
- [20] P. Sunnergren, H. Persson, S. Salomonson, S.M. Schneider, I. Lindgren, and G. Soff, *Phys. Rev. A* **58**, 1055 (1998).
- [21] P. Sunnergren (private communication).
- [22] P.V. Coveney and P.G.H. Sandars, *J. Phys. B* **16**, 3727 (1983).
- [23] H. Backe, R. Engfer, U. Jahnke, E. Kankeleit, R.M. Pearce, C. Petitjean, L. Schellenberg, H. Schneuwly, W.U. Schröder, H.K. Walter, and A. Zehnder, *Nucl. Phys. A* **189**, 472 (1972).
- [24] R. Engfer, H. Schneuwly, J.L. Vuilleumier, H.K. Walter, and A. Zehnder, *At. Data Nucl. Data Tables* **14**, 509 (1974).
- [25] M.G.H. Gustavsson and A.-M. Mårtensson-Pendrill, *Phys. Rev. A* **58**, 3611 (1998).
- [26] E.B. Baker and L.W. Burd, *Rev. Sci. Instrum.* **34**, 238 (1963).
- [27] P. Raghavan, *At. Data Nucl. Data Tables* **42**, 189 (1989).
- [28] A. Lurio and A.G. Prodell, *Phys. Rev.* **101**, 79 (1956).
- [29] A.-M. Mårtensson-Pendrill, *Phys. Rev. Lett.* **74**, 2184 (1995).
- [30] J.E. Rosenthal and G. Breit, *Phys. Rev.* **41**, 459 (1932).
- [31] M.F. Crawford and A.L. Schawlow, *Phys. Rev.* **76**, 1310 (1949).
- [32] H.J. Rosenberg and H.H. Stroke, *Phys. Rev. A* **5**, 1992 (1972).
- [33] T. R. Fowler, Ph.D. thesis, Lawrence Radiation Laboratory, University of California, Berkeley, California, 1968.